



Multi-cell hydrogen storage devices with extra volumetric capacity

R. Du^a, P. Zhang^a, G. Xu^{b,*}

^a Institute of Precision Engineering, The Chinese University of Hong Kong, Shatin, Hong Kong SAR, China

^b Department of Materials Science and Engineering, McMaster University, 1280 Main Street West, Hamilton, Ontario, Canada L8S 4L7

ARTICLE INFO

Article history:

Received 8 August 2008

Received in revised form 7 September 2008

Accepted 8 September 2008

Available online 19 September 2008

Keywords:

Hydrogen storage

Pressurized container

Multi-cell

Volumetric capacity

ABSTRACT

Hydrogen storage remains as a major challenge to the future hydrogen economy. Among the existing methods, pressurized containers are the closest to practical applications. However, their safety concerns, stringent material requirements and high costs are difficult to fulfill simultaneously. Instead of single chamber cylinders, multiple cell structures are proposed here. It is found that such structures offer not only improved safety but also extra storage capacity. This may lead to the practical design and manufacturing of compact hydrogen storage devices that are suitable for portable fuel cell applications, even without employing costly materials.

© 2008 Elsevier B.V. All rights reserved.

1. Introduction

The development of fuel cell technologies calls for safe, light-weight and cost-effective hydrogen storage containers in order to generate environmentally friendly power for mobile or portable applications. As a key component of fuel cell systems, hydrogen storage should meet the targets set by the US Department of Energy (DOE) of 62 kg m^{-3} volumetric density and 6.5% weight density, which are based on the current gasoline storage tank measurements [1]. These numbers remain as the bottleneck toward the hydrogen economy, since none of the existing technologies offer a satisfactory answer. A closer examination of the available methods, such as pressurized vessels, liquefied hydrogen storage, physisorption, intercalation in metals and complex hydrides and storage based on chemical reactions, leads to the observation that, although none of them are currently capable of reaching the US DOE targets, some of them are obviously more advantageous than the others and are much closer to the practical applications [2].

For example, in the case of liquefied hydrogen [3], although it offers satisfactory densities, a cryogenic tank set at 21 K boils off a certain percent of its content daily, since the thermal insulation is not perfect, which not only introduces a huge waste of energy but also produces a hazardous environment, in addition to the large amount of energy needed to liquefy the gas in the first place

[4–6]. For the much studied physisorption and metal hydride systems, they are mainly based on van der Waals interactions between the host and hydrogen molecules. While physisorption requires very large specific surface areas [7–10], the metal hydrides call for the intercalation of hydrogen atoms into interstitial sites [11–13]. Although they offer a higher volumetric density than the requirement, the weight density has been limited to a mere 1–2%, far below the DOE target. Finally, complex hydrides only give off hydrogen at elevated temperatures [14–16], and the chemical reaction-based compounds are not directly reversible [17], despite their superior densities.

Therefore, pressurized containers are the only method left, which has been in operation on testing fuel cell vehicles all over the world and remains as the closest to practical applications today. According to the phase diagram of hydrogen [3], the volumetric density is closely related to the pressure of the hydrogen gas, which is often set at above 700 atm, or 70 MPa. However, since the current state-of-art design is usually based on single cells of cylindrical form, such a high pressure raises safety concerns, when any small crack on the vessel devastates the surroundings. Moreover, their stringent material strength requirements, often achieved by complex techniques involving winding carbon fiber plus metal matrix, are not economically viable. It is therefore the purpose of this paper to develop a better method, and hopefully a smarter structure, which will at least alleviate the stringent requirements of the vessel materials. Such a small step forward may trigger large-scale progress toward the development of the hydrogen economy, especially when the targets are not too far ahead.

* Corresponding author. Tel.: +1 905 525 9140; fax: +1 905 528 9295.
E-mail address: xugu@mcmaster.ca (G. Xu).

2. Proposed method

Following straightforward mechanics, when the size of a cylinder shrinks, the stress loading on its wall is also reduced in proportion, if a constant gas pressure is maintained inside the cylindrical vessel. In particular, we have the following relationship for the thin wall containers [18]:

$$t = \frac{Pr}{\sigma} \quad (1)$$

where σ is the tensile stress loading on the cylinder wall, P is the gas pressure and r and t are the radius and thickness of the container, respectively. Thus, under the same yield strength of a certain material, the maximum storage pressure can easily be tuned by the geometry, i.e., the ratio of radius over thickness. Also, it is obvious that a thicker wall or a thinner cylinder allows for reduced materials strength, while a certain pressure is retained. To achieve the required capacity with thin cylinders, one may stack them up to form a multiple tubular bundle. In so doing, the potential hazard can be minimized, since the amount of hydrogen released by one cracked tube out of a bundle is much reduced.

Another added benefit comes when spherical shaped cells are introduced, since the stress load on the skin of a spherical cell is only half of that of a cylinder, i.e.:

$$t = \frac{Pr}{2\sigma} \quad (2)$$

where r and t are still the radius and wall thickness of the sphere. This brings in a tremendous amount of saving in materials, which is highlighted by a “gain” in storage capacity, in terms of weight density and related volumetric density. One may argue that the very “gain” can simply be collected by a single spherical vessel. However, such geometry does not fit in most practical environments (which is why, under most circumstances, a single chamber cylinder, instead of a spherical vessel, is used). Therefore, it is beneficial again to stack-up smaller spheres, in order to achieve this gain. One last consideration in the scheme is possible additional materials savings by the sharing of a “common wall” during the stack-up, which may be related to the process of removing extra materials found in between the tubes or spheres, due to the less than unity filling factors.

Based on the arguments above, we will first introduce the “gain” plot, to give a clear comparison between the new scheme and the current technology and to highlight the improvement by extra storage capacity versus that from single chamber cylinders, which are assumed to be very long, with negligible amounts of end cap materials. Three testing geometries of multi-cells are considered: cylinders, spheres and cubes (Section 3.1). Finite element analysis (FEA) of the loading stresses (represented by von Mises equivalent stresses) is carried out to verify the three designs. To illustrate the point, our calculation is based on an easily accessible aluminum alloy, which has a maximum tensile strength of about 450 MPa [19]. However, the calculations are independent of the choice of materials (Section 3.2). Finally, further considerations and options are discussed (Section 3.3).

3. Results and discussion

3.1. The “gain” plot

To highlight the increase of hydrogen storage capacity created by a multi-cell structure, a “gain” plot is used to show the volumetric density versus the weight density, traced out by varying pressure, where the “gain” is simply judged by the comparison of the *distances away from the origin* for the various designs. This indicates

the simultaneous maximization of both the volumetric and weight densities. To illustrate the point, the plot is based on a common aluminum alloy (type 2014), with a density of 2700 kg m⁻³ and tensile strength of 450 MPa, whose more detailed properties are obtainable from the Materials Handbook [19]. The temperature is fixed at 298.15 K, and pressure P varies from 0 to 600 MPa.

The volumetric density d_v and gravimetric density d_g of a multi-cell structure are then calculated by

$$d_v = \frac{m_{\text{gas}}}{V_{\text{all}}} = \frac{\rho_{\text{gas}}V_{\text{gas}}}{V_{\text{all}}} \quad (3)$$

$$d_g = \frac{m_{\text{gas}}}{m_{\text{all}}} = \frac{\rho_{\text{gas}}V_{\text{gas}}}{\rho_{\text{gas}}V_{\text{gas}} + \rho_{\text{container}}V_{\text{container}}} \quad (4)$$

where m , V and ρ are the mass, volume and density, respectively. $\rho_{\text{gas}} = m_{\text{H}_2}P/RT(1 + kP)$ is the gas equation of compressed hydrogen, modified from the ideal gas law, with $R = 8.31 \text{ J mol}^{-1} \text{ K}^{-1}$ and $k = 7.1 \times 10^{-9} \text{ Pa}^{-1}$. The volume of a single cylindrical cell is given by $V_{\text{gas}} = \pi r^2 l$, where l is the length of the cylinder and N is the number of cells. Under a fixed radius of a cylindrical cell, the wall thickness t is calculated from:

$$t = \frac{Pr}{\sigma - 0.6P} \quad (5)$$

which is a modified version of Eq. (1), when taking into account the finite wall thickness [18]. To maximize the “gain”, the materials between cells should be minimized as much as possible in order to reduce the weight. Therefore, the cylindrical cells are stacked in hexagonal form, which leads to the calculation of the $V_{\text{container}}$ by

$$V_{\text{container}} = V_{\text{all}} - V_{\text{gas}} = \frac{3\sqrt{3}}{2}r_{\text{out}}^2l - N\pi r^2l \quad (6)$$

where $r_{\text{out}} = (2n - 1)r + nt + 0.1547(r + t)$, with n being the number of cell layers from the center and N being the total cell number: $N = 3n^2 - 3n + 1$. To begin with, the wall thickness t is shared between the neighboring cells, as calculated from Eq. (5).

Based on the above, the resulting “gain” plot is shown in Fig. 1. Under variable pressure, both the volumetric and gravimetric densities first increase and then decrease. The maximum “gain”, compared with the single chamber design, is achieved when the pressure reaches about 100 MPa (1000 atm), signified by the farthest point away from the origin of the plot. Fig. 1 also presents the benefit of using the shared walls, which is shown by a higher gain at larger n numbers. This increase, however, is saturated at about $N = 29,701$ ($n = 100$), due to the presence of “wasted materials” between the cylindrical cells, which then cancels the gain at a too high an n .

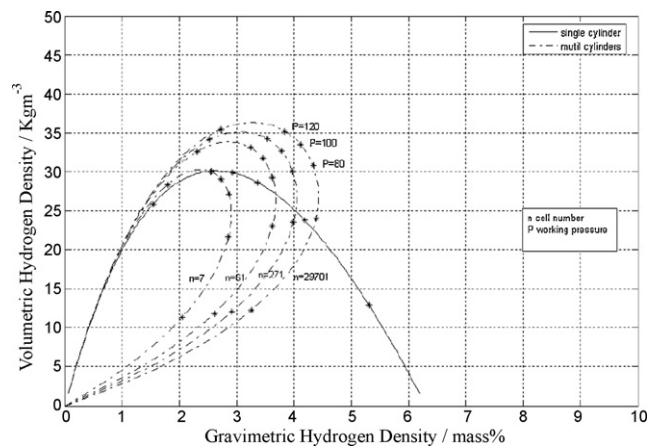


Fig. 1. Gain plot: volumetric and gravimetric densities of single cylinder versus multi-cylindrical cells.

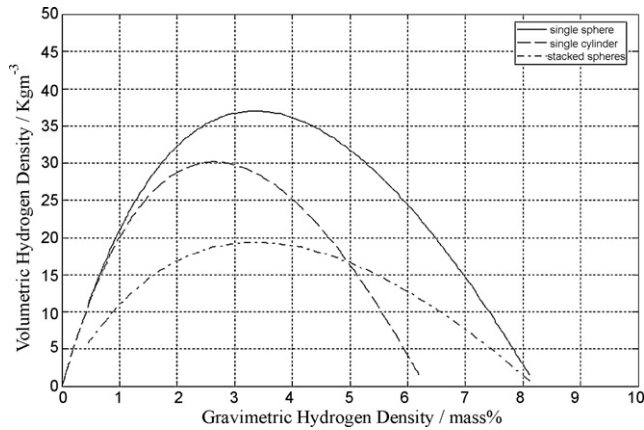


Fig. 2. Gain plot: volumetric and gravimetric densities of single cylinder, single sphere and multi-spherical cells.

The same can be done to the multiple spherical cells. As mentioned above, the stress loading of a spherical cell is only half of that of a cylinder under the same pressure. Therefore, the volumetric and gravimetric densities can be even higher. Using the same scale, Fig. 2 shows the volumetric and gravimetric density curves of a single sphere versus those of a stack of multiple spheres. Surprisingly, there is no benefit shown by the stacked spheres, which give even lower numbers than that of single chamber cylinders. A closer examination reveals the cause, which is attributed to the “wasted” materials in between the spheres. Therefore, unless a “hollow” structure could easily be manufactured, such a scheme does not seem to be beneficial.

To improve the situation, one may use cubes instead of spheres. Fig. 3 shows the resulting volumetric and gravimetric densities of a single cylinder and multiple cubes. It is now evident that the multiple cubic structures have much higher volumetric and gravimetric densities and thus a larger gain from the single chamber cylinder. To strengthen the structure, the outer wall thickness is increased by 2.5 times that of the inner wall, t , which is again calculated from Eq. (2). That is why the gain becomes negative for a small n . Between $n=4$ and $n=125$, there exists a “break-even point”, which means the “saved” material inside is offsetting the “loss” from the extra outer wall. After that, the gain increases with the cell number. At $n=10^6$ and a pressure of 100 MPa, the volumetric density reaches 35 kg m^{-3} , which offers a 15% increase from that of the single chamber cylinder. This is significant as the volumetric density is more

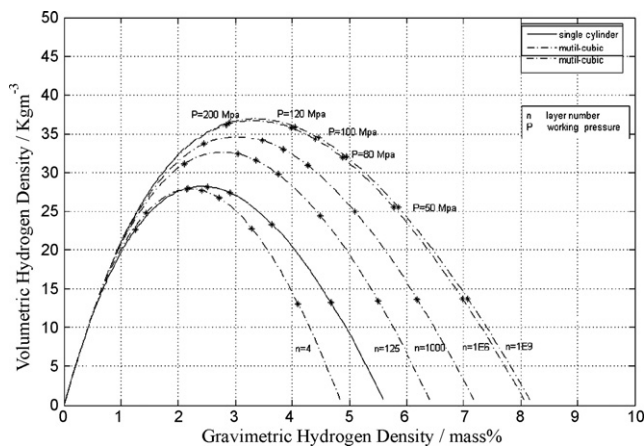


Fig. 3. Gain plot: volumetric and gravimetric densities of single cylinder and multi-cubes.

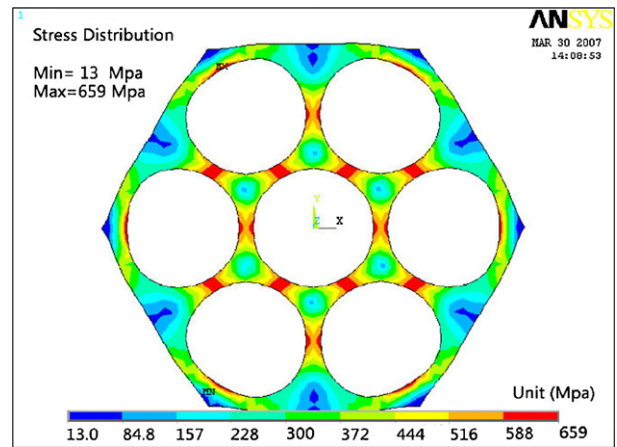


Fig. 4. FEA result: von Mises stress of seven cylindrical cells with $t^* = Pr/\sigma - 0.6P$.

difficult to improve than the weight density. As expected, the gain eventually saturates at higher cell numbers.

3.2. Finite element analysis of multi-cell structure

The gains obtained from multi-cell structures shown by Figs. 1–3 are mainly based on simple calculations of pressure–stress relations (Eqs. (1)–(5)). To further validate the design, we need to analyze the detailed stress loading. This is done by FEA, using software systems of ANSYS. To begin with, we examine seven multi-cylindrical cells, arranged in a hexagonal shape as shown in Fig. 4. Based on the same measures as those given in Section 3.1, viz., a much longer length than the radius, a simple two-dimensional analysis becomes sufficient. Under an internal pressure loading of 100 MPa, as shown in Fig. 4, the von Mises stress at certain areas becomes 50% higher than the tensile strength of the material (450 MPa). This means the design would not be able to survive. To resolve the problem, as shown in Fig. 5, we increase the inner wall thickness by 1.5 times the original t and change the hexagonal outer shape to become circular. The resulting von Mises stress is now reduced to a similar level of the tensile strength of the material. However, in the meantime, as shown in Fig. 6, the new design has a large drop in gains of volumetric and weight densities. Therefore, the gain illustrated by multi-cylindrical cells shown in Fig. 1 has to be achieved in practice by a higher strength material than the selected aluminum alloy.

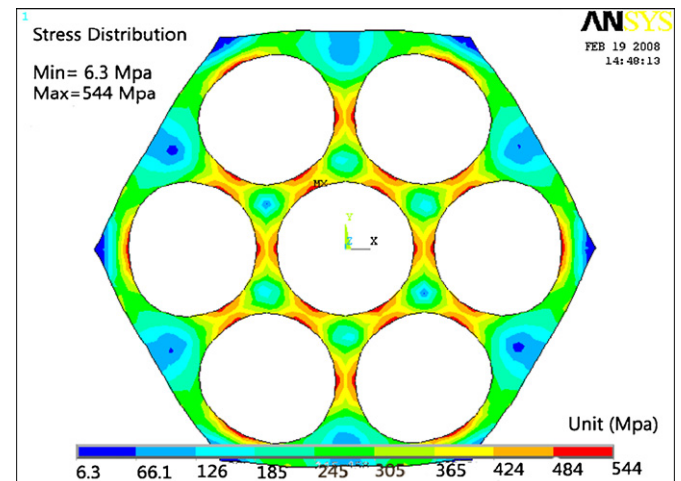


Fig. 5. FEA result: von Mises stress of seven cylindrical cells with $t = 1.5t^*$.

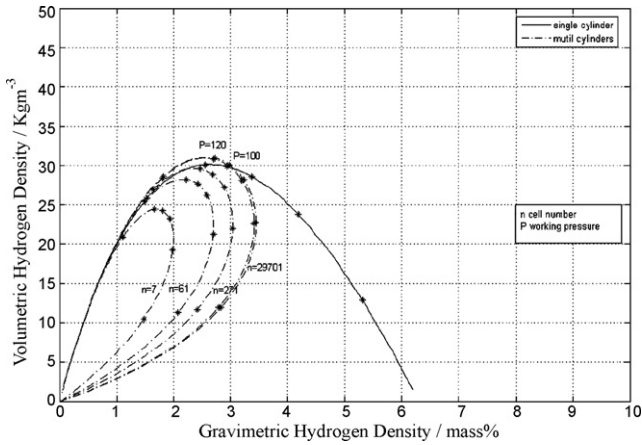


Fig. 6. Gain plot: volumetric and weight densities of multi-cylindrical cells with $t = 1.5t^*$.

Further attempts could be made to balance the gain and the maximum stress loading by fine tuning the structures so that the stress loading does not jeopardize the volumetric and gravimetric density advantage.

In the usual cases, it is fairly uncommon to have cubic or rectangular pressure vessels because of their complex stress distribution. There are not only membrane stresses but also bending stresses, which were non-significant in cylindrical or spherical forms. Worse off, the bending stress is sometimes 10 times larger than the membrane stress. For this reason, stay bars were proposed to stabilize the single cubic structure [20]. Our multi-cubic structure actually resolves the problem in a better way, since the walls of inner cubes are pressurized from both sides, so the bending stresses cancel each other out between the cubes. All that remains is for the outer cubes to be strengthened by extra materials. In the simplest case, as shown in Fig. 7, 27 cubes are stacked up, using the same thickness calculated from Eq. (2), except for the outer wall, which has 2.5 times the thickness. With slightly rounded corners and side edges, and a loading pressure of 100 MPa, the FEA results are shown in Figs. 8–10 for various cells. Overall, the maximum stress now falls within the material strength of the chosen aluminum alloy. As expected for the inner cubes, the pressure acts on both sides of the wall, leading to a cancellation of the loading. For the outer cells, three cases are considered separately: (1) the cube in the center of the outer surface; (2) the cube located at the middle of an edge; and (3) the one at the outer corner. Fig. 8 shows the von Mises stress of

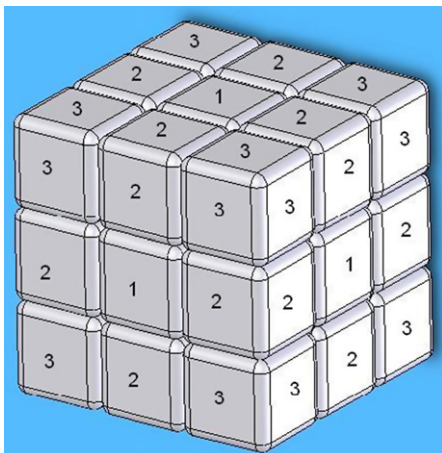


Fig. 7. Illustration of the multi-cubic cell structure.

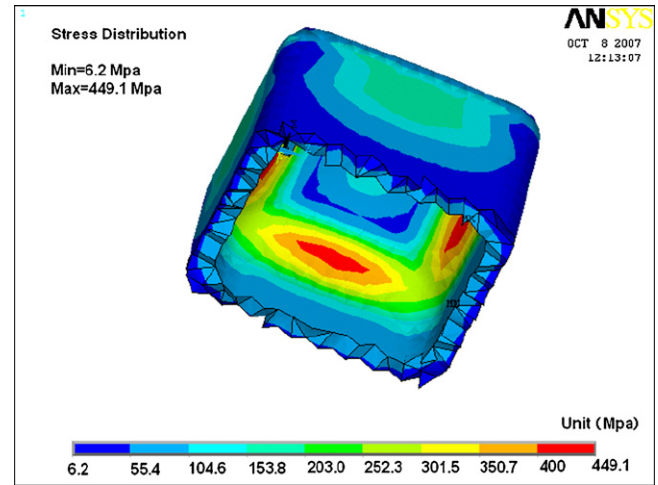


Fig. 8. FEA result: von Mises stress of the cube at the center of the outer layer.

the first case. The maximum stress is 449 MPa, which is less than the materials strength. Note that the maximum stress loading occurs at the middle of the internal surface, in agreement with the theoretical calculation. Fig. 9 shows the stress distribution of the second case, in which two outer walls are thickened. The maximum stress is still acceptable. Fig. 10 shows the stress distribution of the cube at the corner, in which three outer walls of the cube are thickened. The maximum stress is again within the limits. Therefore, the design is successful with a sizable gain in storage densities.

3.3. Discussion

Our analysis has been mainly based on the geometry (single to multi-cells) of the structures, which is obviously independent of the choice of materials. Although we have used a low-cost aluminum alloy in the calculation, it is actually advantageous to employ better materials with higher tensile stress and lower weight, which will certainly enable us to achieve still better performance. For example, a commonly used material for pressurized hydrogen storage is winding carbon fiber composite. The aerospace-grade carbon fiber has a tensile stress of 3500 MPa and a density of 1500 kg m⁻³ [19]. With that material, the state-of-art performance achieved by single chamber cylinders, such as that achieved by Quantum's 10,000 psi (70 MPa) TriShield™ tank, already gives a

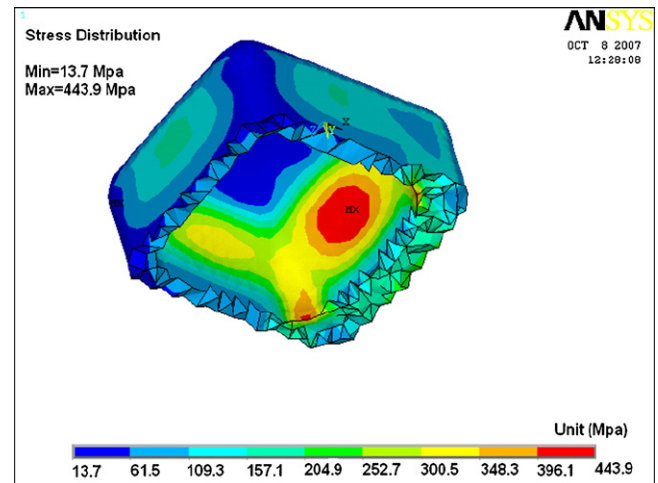


Fig. 9. FEA result: von Mises stress of the cube at the edge of the outer layer.

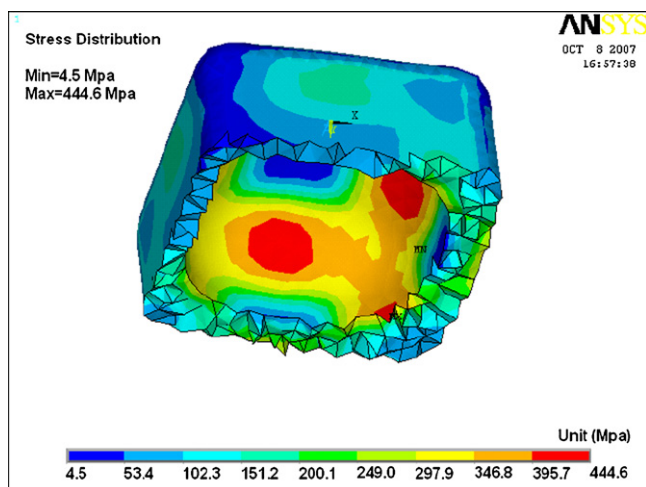


Fig. 10. FEA result: von Mises stress of the cube at the corner of the outer layer.

specific energy of 1.75 kWh kg^{-1} , a short fall below the DOE 2010 target of 2 kWh kg^{-1} [21]. Using our design, it is obvious that the 15% gain will easily fill the remaining gap. Taking the cost issue into account, the aluminum alloy becomes a good choice with a reasonable tensile strength, which also enables the development of storage devices for portable applications.

Similar work can also be performed on other forms of multi-cell configurations than the spherical and cubic, since the spherical structure offers low storage densities (as shown in Fig. 2), and the cubic has non-uniform stress distribution. One example is the polyhedron cell, which fills the space seamlessly (Fig. 11). This is called the Kelvin structure [22], as shown by Fig. 12. It has six square facets and eight hexagon facets. The volume of a Kelvin cell is calculated by $8\sqrt{2}a^3$, where a is the length of a straight edge. Obviously, it has a similar surface to volume ratio to that of a sphere, yet it involves no wasted space or material during stacking. Thus, it is expected to have a higher gain than the multi-spheres but with less un-even stress distribution than the multi-cubes, combining the advantages from both structures.

In practice, there will be channels/holes connecting the cells for the hydrogen gas to go through. The channels/holes should be located at the face-center of the cubes, because, from Figs. 8–10, we learn that the loading stress reaches a minimum there. The diameter of the holes should be small enough in order not to affect the strength of the structure [18] but large enough to allow the efficient transport of gas molecules. The latter can be judged by the mean

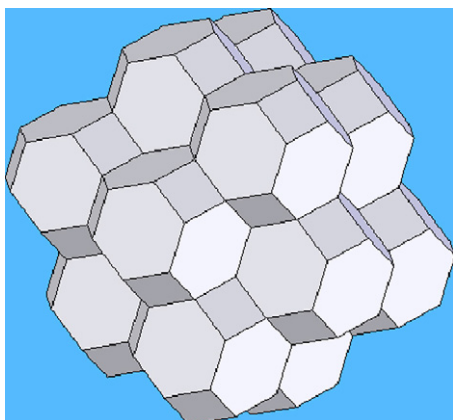


Fig. 11. Illustration of a Kelvin polyhedron cell.

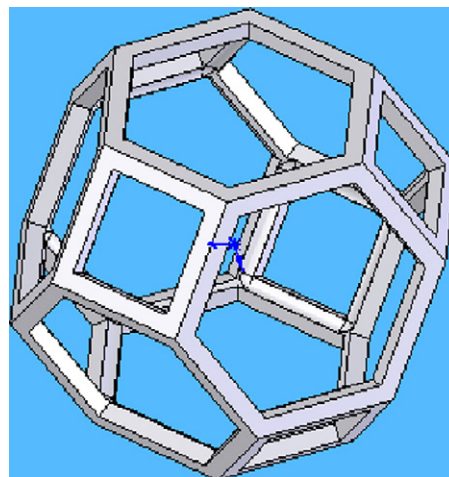


Fig. 12. Stacks of Kelvin polyhedron cells.

free path of the gases. If the gas pressure is set at about 100 MPa ($\sim 1000 \text{ atm}$), the mean free path, λ , is only about a dozen nanometers. The hole diameter, L , can then be chosen so that the Knudsen number ($K_n = \lambda/L$) is small, to avoid the rare gas phenomenon [23]. If one cell is punctured or ruptured, due to the small connecting holes, the gas in the remaining chambers will be released much more slowly than that of a single chamber design. That offers improved safety for the multiple cell structure. In the meantime, for a given weight or volume of fuel tank and a given operating pressure, a higher margin of safety over the yield point of the materials is achieved.

4. Conclusions

To find a better method of hydrogen storage, two types of multi-cell structures for compressed hydrogen are analyzed here. While the cylindrical multi-cell structure has some limitations, the cubic multi-cell structure offers a high amount of gain in storage capacity using the same materials. The multi-cell structures not only outperform the single cylindrical structure but also offer an opportunity to reduce risks in portable fuel storage systems, which ensures a more rapid development of smart structures of pressurized hydrogen storage.

References

- [1] The website of US Department of Energy (2007) <http://www.eere.energy.gov/>.
- [2] A. Züttel, Mater. Today (September 2003) 24–33.
- [3] D.R. Lide (Ed.), Handbook of Chemistry and Physics, 85th ed., CRC Press, Boca Raton, 2004, pp. 6.16–6.17.
- [4] T.M. Flynn, in: S.P. Parker (Ed.), McGraw-Hill Encyclopedia of Science & Technology, 7th ed., McGraw-Hill, New York, 1992, pp. 106–109.
- [5] G. Chen, S. Anghaie, NASA/NIST databases (2007) http://www.inspi.ufl.edu/data/h_prop-package.html.
- [6] M. von Ardenne, G. Musiol, U. Klemradt (Eds.), Effekte der Physik, Verlag Harri Deutsch, Frankfurt am Main, 1990, pp. 712–715.
- [7] M. Rzepka, P. Lamp, M.A. de la Casa-Lillo, J. Phys. Chem. B 102 (1998) 10849–10898.
- [8] R. Ströbel, L. Jorissen, T. Schliermann, V. Trapp, W. Schütz, K. Bohmhammel, G. Wolf, J. Garcke, J. Power Sources 84 (1999) 221–224.
- [9] C. Nützenadel, A. Züttel, L. Schlapbach, in: H. Kuzmany, J. Fink, M. Mehring, S. Roth (Eds.), Science and Technology of Molecular Nanostructures, American Institute of Physics, New York, 1999, pp. 462–465.
- [10] N.L. Rosi, J. Eckert, M. Eddaoudi, D.T. Vodak, J. Kim, M. O'Keeffe, O.M. Yaghi, Science 300 (2003) 1127–1129.
- [11] G.R. Pearson, Chem. Rev. 85 (1985) 41–49.
- [12] Y.Z. Fukai, Phys. Chem. 164 (1989) 163–165.
- [13] P. Rittmeyer, U. Wietelmann, Ullmann's Encyclopedia of Industrial Chemistry, vol. A13, 5th ed., Wiley-VCH, Weinheim, 1996, pp. 199–226.

- [14] B. Bogdanovic, R.A. Brand, A. Marjanovic, M. Schwickardi, J. Tolle, J. Alloys Compd. 302 (2000) 36–58.
- [15] A. Züttel, P. Wenger, S. Rentsch, P. Sudan, Ph. Mauron, Ch. Emmenegger, J. Power Sources 118 (2003) 1–7.
- [16] S.J. Lippard, D.A. Ucko, Inorg. Chem. 7 (1968) 1051–1056.
- [17] A. Steinfeld, Int. J. Hydrogen Energy 27 (2002) 611–619.
- [18] J.R. Farr, M.H. Jawad, Guidebook for the Design of ASME Section VIII: Pressure Vessels, 2nd ed., ASME Press, New York, 2001, pp. 27–29, 186–199, and 136–153.
- [19] A.H. Charles (Ed.), Handbook of Materials for Product Design, McGraw-Hill, New York, 2001, pp. 2.18–2.77.
- [20] S.M. Aceves, A. Weisberg, F. Espinosa-Loza, S. Perfect, G. Berry, DOE Hydrogen Program FY 2005 Progress Report, VI.E.2 Advanced Concepts for Containment of Hydrogen and Hydrogen Storage Materials (2007) http://www.hydrogen.energy.gov/pdfs/progress05/vi_e_2_aceves.pdf.
- [21] J. Ko, K. Newell, B. Geving, W. Dubno, DOE Hydrogen Program FY 2005 Progress Report, VI.E.1 Compressed/Liquid Tanks (2007) http://www.hydrogen.energy.gov/pdfs/progress05/vi_e_1_ko.pdf.
- [22] Lord Kelvin, Philos. Mag. 24 (1887) 503–514.
- [23] G.E. Karniadakis, A. Beskok, Micro Flows: Fundamentals and Simulation, Springer, New York, 2002, pp. 1–31.